Applied Physics Letters ARTICLE scitation.org/journal/apl

Dipole-relaxation dynamics in a modified polythiourea with high dielectric constant for energy storage applications

Cite as: Appl. Phys. Lett. **115**, 163901 (2019); doi: 10.1063/1.5123484
Submitted: 6 August 2019 · Accepted: 6 October 2019 ·

Chao Wu,[1,2] Zongze Li,[1,2] Gregory M. Treich,[3] Mattewos Tefferi,[1,2] Riccardo Casalini,[4] Rampi Ramprasad,[5] Gregory A. Sotzing,[3] and Yang Cao[1,2,a)]

AFFILIATIONS

[1]Electrical Insulation Research Center, Institute of Materials Science, University of Connecticut, Storrs, Connecticut 06269, USA
[2]Department of Electrical and Computer Engineering, University of Connecticut, Storrs, Connecticut 06269, USA
[3]Polymer Program, University of Connecticut, Storrs, Connecticut 06269, USA
[4]US Naval Research Laboratory, Washington, DC 20375, USA
[5]School of Materials Science and Engineering, Georgia Institute of Technology, Atlanta, Georgia 30332, USA

[a)]**Email:** yang.cao@uconn.edu

ABSTRACT

Enhancing dipole polarization has been demonstrated as an effective approach to increase the dielectric constant of polymer dielectrics and thus to improve their discharged energy density for energy storage applications in electrical power and electronic systems. However, further optimization to get a higher dielectric constant and lower polarization loss hinges upon a more insightful understanding of the dynamics of dipole relaxation. Here, we demonstrate an approach, based on the Dissado-Hill dielectric response model, to probe the dynamics of dipole polarization in an all organic polythiourea (PDTC-HK511) composed of p-phenylene diisothiocyanate (PDTC) as rigid segments and Jeffamine® HK511 as flexible segments. Our results reveal that PDTC-HK511 possesses strong subglass transition β and γ relaxation processes in conjunction with the quasi-DC diffusion process at relatively high temperature and a low frequency range. The γ relaxation enhances the dielectric constant by 20%–25% but causes no apparent loss at the operating temperature and frequency conditions due to the high flexibility and short relaxation time of the dipole orientation. In comparison to β relaxation, the weak interactions and much shorter relaxation time of dipoles in γ relaxation evidenced the large flexibility of dipole movement. This work provides deeper insight into the dipole movement and aids future rational designs of polymers for dielectric energy storage.

Dielectric energy storage is of significance for electrical power and electronic systems, owing to the high discharged energy density and ultrafast charging-discharging rate.[1–6] The rising demands in the development of grand electrical systems and ultracompact electronic devices require dielectric materials with higher energy density.[1,3–7] Energy density is determined by the dielectric constant and the applied electric field, which means that when operated at the same electric field, the dielectric constant will be the most dominant factor. Compared to its counterparts such as ceramic and electrolytic capacitors, polymer film capacitors are favored for their high voltage scalability, high ripple current handling, and graceful failure behavior.[8,9] However, further adoption of polymer film capacitors is limited by the relatively low dielectric constant of polymers in comparison with those of ceramic dielectrics.[10,11] For this reason, polymer composite dielectrics have been developed to increase the dielectric constant, but this is often achieved at the cost of compromised breakdown strength and film processability.[12,13] It is desirable to develop all-organic polymers with a high dielectric constant and low polarization loss.

To address these issues, researchers explored polymers with strong polar groups to obtain a high dielectric constant in different stereostructures. The ferroelectric fluorine polymer poly(vinylidene fluoride) (PVDF) and its copolymers have been considered as dielectric candidates owing to their high dielectric constant. However, the large remnant polarization and hysteresis loss arising from the large scales of movement of dipolar segments hampered their further applications.[14,15] Consequently, polymers with rigid backbones were synthesized to constrain the large-scale movements of polymer chains and hence to decrease the resulting loss.[4,16,17] As fully rigid backbones also made it more difficult for dipoles to reorient along with the applied electric field, we previously proposed the concept of linking the rigid segments with flexible chains so as to locally improve the flexibility of dipoles.[18] All of these approaches could benefit from a more insightful understanding of the dipolar relaxation processes such that further optimization of the polymer structures can be carried out with rational designs. Hence, it is highly imperative to probe the physical characters of the dipole movement related to the microstructure of the polymer.

In this work, we present a method to obtain the characteristics of the dynamics of dipole relaxation based on the Dissado-Hill model.[19–24] Compared to the empirical models such as Cole-Cole function, Davidson-Cole function, and Havriliak-Negami function, the response function in the Dissado-Hill model can be correlated with the physical nature of the material structure and charge dynamics.[21,22,25] Here, the model polymer is a rigid p-phenylene diisothiocyanate (PDTC) linked by the flexible linear Jeffamine® HK511, referred to as PDTC-HK511, as illustrated in Fig. 1(a). The rigid segments from PDTC are introduced to provide a high glass transition temperature ($T_g = 92\,^\circ\mathrm{C}$ as determined by differential scanning calorimetry) and a thermally stable structure. The flexible chains from Jeffamine® HK511 are introduced to increase the movement flexibility of dipoles. More details about the synthesis can be found in our previous work.[18] The thickness of the PDTC HK511 film is ∼10 μm, determined by using a thickness gauge with a guaranteed absolute accuracy of 0.2 μm (Model LE1000–2, Measure It All) as the average of five measurements. Dielectric spectroscopy was performed using a Novocontrol Broadband Dielectric Spectrometer with a Quatro Cryosystem on films metallized with sputter coatings of Au/Pd.

The dielectric response of PDTC-HK511 was investigated in a wide frequency range of 10^{-2}–10^{6} Hz and temperature range of $-130 \sim 70\,^\circ\mathrm{C}$, which is below its glass transition temperature, as presented in Figs. 1(b)–1(d). The imaginary part of the relative permittivity represents the dielectric loss of PDTC-HK511. Two kinds of relaxations, each with an obvious peak in dielectric loss, can be clearly identified, namely, the γ relaxation and β relaxation. As γ relaxation is formed by the site reorientation of dipoles and β relaxation is a result of the localized movement of polymer chains with polar groups,[26,27] the greater site-flexibility made the γ relaxation appear in higher frequency and lower temperature ranges relative to the β relaxation. In addition to the β and γ relaxation, another response process can be found in PDTC-HK511 at elevated temperatures approaching its glass transition temperature, whereby both the real part and imaginary part of the relative permittivity increase as frequency decreases, as illustrated in Fig. 1(d). The observed response process is a quasi-DC (Q-DC) dispersion process.[22] It should be noted that the improvement of the dielectric constant at a relatively low frequency and high temperature arising from the Q-DC process has no significance for energy storage as it is always accompanied by high dielectric loss.

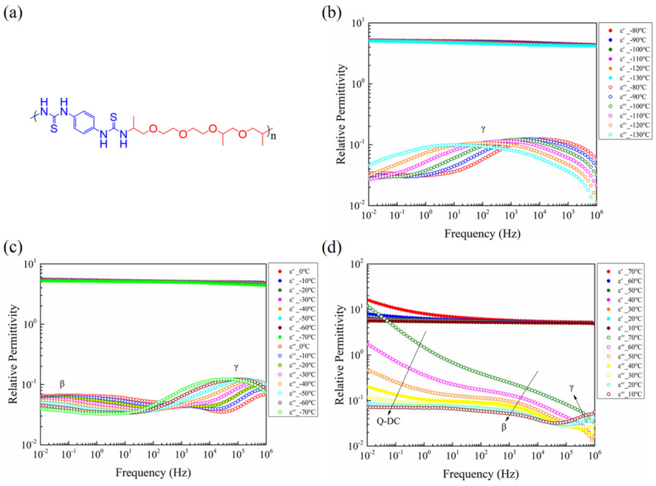

FIG. 1. (a) Chemical structure of the model polymer PDTC-HK511; dielectric spectroscopy of PDTC-HK511 in the temperature range of (b) $-130 \sim -80\,^\circ\mathrm{C}$, (c) $-70 \sim 0\,^\circ\mathrm{C}$, and (d) $10 \sim 70\,^\circ\mathrm{C}$. The solid circles represent the real part of the complex relative permittivity, and the open circles represent the imaginary part of the complex relative permittivity. Curves with characteristics of γ relaxation, β relaxation, and Q-DC process are marked in the figures.

Two types of basic charge dynamics were characterized in the Dissado-Hill dielectric response model. For dipoles (or bonded charge pairs), the orientation of them formed response processes with a peak in the loss as frequency changes, like the β and γ relaxation here. The real part becomes approximately constant at low frequencies well below that of the loss peak. The response function is described by the following equation:[21]

$$\chi^*(\omega) = \chi_0 \frac{\Gamma(1+m-n)}{\Gamma(2-n)\Gamma(m)} \left(1 + i\frac{\omega}{\omega_p}\right)^{n-1} \times {}_2F_1\left(1-n, 1-m; 2-n; \left(1 + i\frac{\omega}{\omega_p}\right)^{-1}\right), \tag{1}$$

where $\chi^*(\omega)$ is the complex susceptibility whose real part represents the energy storage and imaginary part represents the loss in dielectric polarization processes. $\Gamma(x)$ is the Gamma function and ${}_2F_1(a, b; c; z)$ is the Gaussian hypergeometric function. Amplitude χ_0 denotes the net concentrations of dipoles formed in the unit electric field. In the dielectric polarization process, the movement of dipoles will interact with their local environment and neighboring dipoles due to the electric force and mechanical steric constraints. That is, the response of dipoles to the applied electric field is a cooperative movement. In the Dissado-Hill model, the interactions of neighboring dipoles were considered using the concept of clusters. At high frequency, the interactions of dipoles occur within the cluster, forming intracluster interactions. At low frequency, the orientation of dipoles would affect the dipoles at a further distance beyond the size of cluster, forming intercluster interactions. For γ relaxation in this paper, the cluster is regarded as the repeating unit of PDTC-HK511. For β relaxation, the cluster is considered to be the local chain segments that have flexibility to reorient. The shape parameters m and n in the response function characterized the intercluster and intracluster interactions, respectively. In the logarithmic coordinate of χ'' and frequency, m is the slope of the low frequency branch and n-1 is the slope of the high frequency branch.

Other than the orientation of dipoles, charges weakly bonded to their counter charge will be separated and move independently. The resulting response is a Q-DC process, which can be described by the following equation:[22]

$$\chi^*(\omega) = \chi_0 \frac{\Gamma(1-p-n)}{\Gamma(1-n)\Gamma(1-p)}\left(1+i\frac{\omega}{\omega_c}\right)^{n-1} \times {}_2F_1\left(1-n,1+p;2-n;\left(1+i\frac{\omega}{\omega_c}\right)^{-1}\right). \qquad (2)$$

In the Q-DC process, the real part of susceptibility is a function of frequency in the low frequency range as further separation of charges will also give rise to the energy storage. The dramatic increase in ε' in Fig. 1(d) revealed the characteristics of the Q-DC process.

With the above observed characteristics, the equivalent circuit of PDTC-HK511 can be built with elements correlated with γ relaxation, β relaxation, and the Q-DC process, together with an infinite frequency component, as illustrated in Fig. 2(a). With the complex capacitance correlated with γ relaxation, β relaxation, and the Q-DC process, energy storage and loss in each process can be quantitatively extracted. ε_∞ denotes the contribution of all relaxation mechanisms in the frequency beyond the measurement frequency window (due to very fast processes such as electronic and atomic polarization).[27] With the equivalent circuit decomposition based on the Dissado-Hill model, the complex susceptibilities of γ relaxation, β relaxation, and the Q-DC process are extracted from the dielectric spectra, as presented in Figs. 2(b)–2(d). Contributions of different relaxations are clearly revealed by various colored curves with each polarization defined in the figures. From Figs. 2(b)–2(d), it can be found that the highest contribution to the dielectric constant arose from ε_∞. Here, ε_∞ is the sum total of the dielectric constant of electronic and atomic polarizations that occurred at very high frequencies ($>10^{11}$ Hz). γ relaxation contributed the second highest to the dielectric constant, as presented in Figs. 2(b)–2(d).

As the calculated power law index p is <0.6, the Q-DC process observed at a relatively high temperature ($>30\,°$C) and low frequency (<1 Hz) range is formed by the anomalous diffusion process in which the typical power law index is in the range of 1/3–2/3.[25,28–30] Therefore, here we focus on the sub-T_g dipolar polarization processes of PDTC-HK511, namely, the γ relaxation and the β relaxation. Using the decomposition of the relaxation processes, the contribution of each individual relaxation at 20 °C to the dielectric constant is summarized in Fig. 3(a). If we consider the atomic and electronic relaxation as the intrinsic polarization, at 20 °C, the contribution of γ relaxation and β relaxation is about 23% and 6% of their total value, respectively.

The dynamics of dipolar relaxation can be summarized through three categories of physical characteristics, which are the rotational speed of the dipoles, the density of the dipoles, and interactions of the adjacent dipoles. As illustrated in Fig. 3(b), with the Arrhenius plot of $\log(f_p)$ vs $1/T$, the activation energy of the relaxation frequency is 0.3 eV for the γ relaxation and 0.85 eV for the β relaxation. The frequency f_p ($=\omega_p/2\pi$) denotes the rotational speed of the dipoles correlated with the maximum polarization loss. f_p of the γ process is much higher than that of the β relaxation, i.e., at $-30\,°$C, f_p of the γ process is $\sim$7 orders of magnitude higher than that of the β process. In general, the operational temperature for energy storage applications is higher than $-50\,°$C, wherein f_p of the γ process is higher than 10^5 Hz. The higher f_p signifies that the orientation of the dipoles responds more quickly to the applied electric field. Combining the plots in Fig. 2(c), the dielectric constant of γ relaxation is almost constant because the γ relaxation is essentially completed once the frequency is lower than 10^3 Hz. In a more usual temperature range, i.e., room temperature, the contribution to the dielectric constant of the γ relaxation will be independent of frequency below 1 MHz. Such a stable contribution to the dielectric constant is of significance for practical applications. In this respect, however, the lower f_p of the β relaxation is not as favorable as is the γ relaxation, resulting in a frequency-dependent (unstable) dielectric constant over the measuring frequency range.

The amplitude χ_0 reflects the density of dipoles reoriented by a unit electric field. First of all, the β relaxation of PDTC-HK511 is not as strong as the γ relaxation, as evidenced by the amplitudes shown in Fig. 3(c). The temperature dependence shown in Fig. 3(c) has a

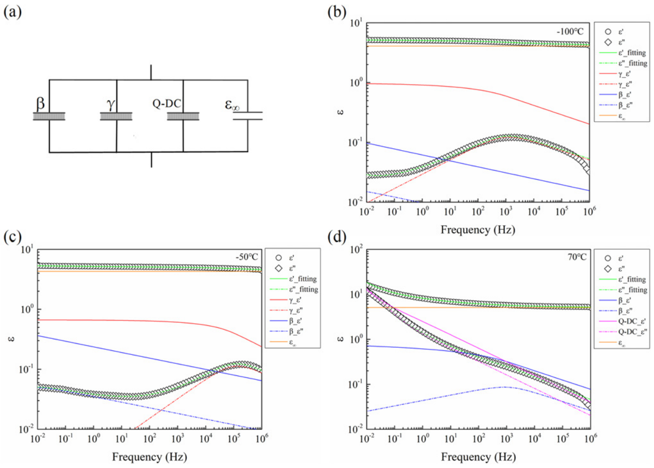

FIG. 2. (a) Equivalent circuit of PDTC-HK511; decomposition of the relaxation processes at (b) $-100\,°$C, (c) $-50\,°$C, and (d) 70 °C. The open circles and diamonds represent the original data. The solid colored lines are the real part and the dashed colored lines are the imaginary part of the susceptibility in each relaxation process.

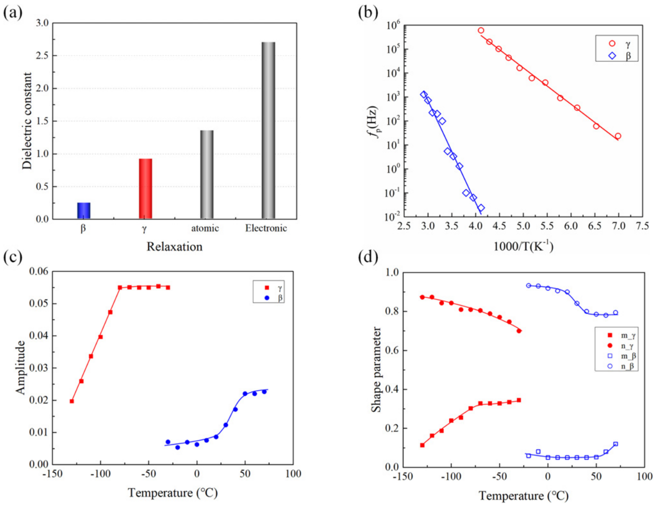

FIG. 3. (a) Contributions of different relaxation mechanisms to the dielectric constant. Atomic and electronic relaxation can be found in Ref. 18 in more detail. (b) Arrhenius plot of the characteristic frequency of the β and γ relaxation; (c) the amplitude of the β and γ relaxation as a function of temperature; and (d) the shape parameters m and n of β and γ relaxations.

sigmoidal form for both γ and β relaxations, i.e., it moves from a high constant value to lower values as the temperature decreased below a specific temperature. This form of behavior of dipoles is indicative of the loss of their ability to reorient due to the steric hindrance of other polymer chains in the surrounding structures below a given temperature. The temperature at which this occurs is much lower for the γ relaxation (reduction for $T < -80\,^\circ C$) than for the β relaxation (reduction when $T < 50\,^\circ C$), which suggests that dipoles involved in the γ relaxation have much more freedom of orientational movement than those of the β relaxation. These amplitude reductions cannot be attributed to the glass transition as it lies at higher temperatures, and there is no indication of a biphasic structural rearrangement in the Arrhenius plot of the peak frequency. The latter fact indicates that the same dipoles reorienting over the same potential barrier are involved in the temperature range investigated. The reduction in amplitude must therefore be associated with the reduction in local chain flexibility due to the steric hindrance of neighboring chains as the temperature is lowered. This would lock some of the dipoles in place so that they are unable to reorient in the field. Such a process would be expected to affect chain segments (β relaxation) at a higher temperature than local bond rearrangements (γ relaxation). Figure 3(c) shows that the restriction of chain segments is essentially completed by $T = 0\,^\circ C$, below which no further reduction occurs, whereas locking the local dipoles involved in the γ relaxation starts at $T = -80\,^\circ C$ and has not been completed by $T = -130\,^\circ C$.

Further insight into the dipole reorientation dynamics is obtained from the shape parameters of the relaxation peaks given in Fig. 3(d). Here, it is clear that the values of power law index n are much higher than those of m, with n lying in the range of 0.7–0.9 and m 0.1–0.3. These values indicate dipoles whose motions are strongly coupled within clusters and whose reorientations are strongly coupled from cluster to cluster, i.e., the relaxation of the dipoles in different clusters is strongly correlated. In this context, it should be noted that $m = 1$ is the same as the $f < f_p$ behavior of the Debye model, which is based on independent dipole relaxations and thus corresponds to essentially independent cluster relaxations. For the γ relaxation, if we consider the cluster as the unit structure of the polymer, the intercluster interaction (index m) arises from the hindrance due to dipoles in neighboring polymer chains or adjacent units. As the β relaxation represents localized movement in larger scales of polymer segments with dipoles, m of β relaxation reflects the interaction between different segments. The intracluster interactions (index n) of both γ and β relaxations cover the same range and therefore indicate a similar degree of correlation, but the intercluster correlations of the γ relaxation are less strong (higher m) than those of the β relaxation, i.e., in the γ relaxation, the dipole cluster relaxations are less connected to other clusters than they are in the β relaxation. This indicates that small local regions have greater flexibility than larger chain segments. The most important point about Fig. 3(d) is, however, that for the β relaxation, there is a step increase in n and a step decrease in m as the temperature drops below $T = 50\,^\circ C$, the same temperature where a step change in amplitude takes place [Fig. 3(c)]. This shows that for the β relaxation, the prevention of a portion of its dipoles from reorientation is accompanied by an increased correlation of the dipole movements. In the case of the γ relaxation, the changes in n and m are not clear-cut. The index m does decrease from a near constant value as the temperature is lowered below $T = -75\,^\circ C$, but the index n seems to increase steadily over the range of $-30\,^\circ C$ to $-130\,^\circ C$. Nevertheless, the changes show a similar trend to those of the β relaxation and occur close to the temperature at which the amplitude starts to decrease [Fig. 3(c)]. The amplitude indicates the density of dipoles being able to reorient. The shape parameters n and m represent the dipole motions within a cluster and over different clusters. It therefore seems that the lowering of energy beneath the rotational energy barrier that prevents some of the dipoles in the γ and β relaxations from being able to reorient along with the electric field also correlates strongly the dipole motions within a cluster and over different clusters. This may arise because the lowered energy state below a relevant onset temperature dipole relaxation can only take place as a result of such correlations.

In summary, we utilized the Dissado-Hill model to analyze the dielectric response and obtained the dynamics of dipolar relaxation in PDTC-HK511. Compared to the intrinsic atomic and electronic polarizations, the subglass relaxations enhanced dielectric constant by 29% at room temperature. The systematic analysis of the dynamics covering the reorientation speed of dipoles, density of dipoles, and interactions of the dipoles as a function of temperature revealed that local bond regions became flexible above $T = -80\,^\circ C$ and thereby increased the contribution of these dipoles to the dielectric susceptibility. Meanwhile, chain segments only became flexible at temperatures above $T = 50\,^\circ C$ to provide additional dipolar polarization contribution to the susceptibility. Altogether, the dielectric constant of the material was considerably increased and the dielectric loss reduced in the service range of temperatures and frequencies as intended from the designed structure of PDTC-HK511. Capable of providing quantitative physical characteristics of dipole relaxation dynamics, the approach demonstrated here presented a powerful guide for the further rational design and optimization of dielectric polymers with a high dielectric constant and low polarization loss for energy storage applications.

The authors are grateful to acknowledge the financial support from a Multidisciplinary University Research Initiative (MURI) Grant (No. N00014-10-1-0944) and a Rational Design of Polymer Dielectrics Grant (No. N00014-16-1-2580), both from ONR. Chao Wu would like to thank Professor Leonard A. Dissado at the University of Leicester for the discussion on physical nature of the dipole relaxation dynamics.

REFERENCES

[1] Q. Tan, P. Irwin, and Y. Cao, IEEJ Trans. Fundam. Mater. **126**, 1153 (2006).
[2] W. Sun, X. Lu, J. Jiang, X. Zhang, P. Hu, M. Li, Y. Lin, C. Nan, and Y. Shen, J. Appl. Phys. **121**, 244101 (2017).
[3] Y. Zeng, Z. Shen, Y. Shen, Y. Lin, and C. Nan, Appl. Phys. Lett. **112**, 103902 (2018).
[4] A. Mannodi-Kanakkithodi, G. M. Treich, T. D. Huan, R. Ma, M. Tefferi, Y. Cao, G. A. Sotzing, and R. Ramprasad, Adv. Mater. **28**, 6277 (2016).
[5] A. F. Baldwin, R. Ma, A. Mannodi-Kanakkithodi, T. D. Huan, C. Wang, M. Tefferi, J. E. Marszalek, M. Cakmak, Y. Cao, R. Ramprasad, and G. A. Sotzing, Adv. Mater. **27**, 346 (2015).
[6] R. Ma, V. Sharma, A. F. Baldwin, M. Tefferi, I. Offenbach, M. Cakmak, R. Weiss, Y. Cao, R. Ramprasad, and G. A. Sotzing, J. Mater. Chem. A **3**, 14845 (2015).
[7] G. M. Treich, S. Nasreen, A. Mannodi-Kanakkithodi, R. Ma, M. Tefferi, J. Flynn, Y. Cao, R. Ramprasad, and G. A. Sotzing, ACS Appl. Mater. Interfaces **8**, 21270 (2016).

[8] Q. Li, F. Liu, T. Yang, M. R. Gadinski, G. Zhang, L. Chen, and Q. Wang, Proc. Natl. Acad. Sci. U.S.A **113**, 9995 (2016).

[9] R. Ma, A. F. Baldwin, C. Wang, I. Offenbach, M. Cakmak, R. Ramprasad, and G. A. Sotzing, ACS Appl. Mater. Interfaces **6**, 10445 (2014).

[10] Y. Wang, L. Wang, Q. Yuan, J. Chen, Y. Niu, X. Xu, Y. Cheng, B. Yao, Q. Wang, and H. Wang, Nano Energy **44**, 364 (2018).

[11] Z. Sun, C. Ma, X. Wang, M. Liu, L. Lu, M. Wu, X. Lou, H. Wang, and C. Jia, ACS Appl. Mater. Interfaces **9**, 17096 (2017).

[12] H. Tang, Z. Zhou, and H. A. Sodano, Appl. Phys. Lett. **104**, 142905 (2014).

[13] Y. Feng, M. Li, W. Li, T. Zhang, Y. Zhao, and W. Fei, Appl. Phys. Lett. **112**, 022901 (2018).

[14] O. N. L. Smith, Y. Kim, M. Kathaperumal, M. R. Gadinski, M. Pan, Q. Wang, and J. W. Perry, ACS Appl. Mater. Interfaces **6**, 9584 (2014).

[15] M. R. Gadinski, K. Han, Q. Li, G. Zhang, W. Reainthippayasakul, and Q. Wang, ACS Appl. Mater. Interfaces **6**, 18981 (2014).

[16] Z. Zhang, D. H. Wang, M. H. Litt, L. Tan, and L. Zhu, Angew. Chem., Int. Ed. **130**, 1544 (2018).

[17] S. Wu, W. Li, M. Lin, Q. Burlingame, Q. Chen, A. Payzant, K. Xiao, and Q. M. Zhang, Adv. Mater. **25**, 1734 (2013).

[18] Z. Li, G. M. Treich, M. Tefferi, C. Wu, S. Nasreen, S. K. Scheirey, R. Ramprasad, G. A. Sotzing, and Y. Cao, J. Mater. Chem. A **7**, 15026 (2019).

[19] L. A. Dissado and R. M. Hill, Nature **279**, 685 (1979).

[20] R. M. Hill and L. A. Dissado, Nature **281**, 286 (1979).

[21] L. A. Dissado and R. M. Hill, Proc. R. Soc. London **390**, 131 (1983).

[22] L. A. Dissado and R. M. Hill, J. Chem. Soc., Faraday Trans. 2 **80**, 291 (1984).

[23] L. A. Dissado, R. C. Rowe, A. Haidar, and R. M. Hill, J. Colloid Interfaces Sci. **117**, 310 (1987).

[24] C. Wu, X. Liang, L. A. Dissado, N. M. Chalashkanov, S. J. Dodd, Y. Gao, and S. Xu, Compos. Sci. Technol. **163**, 56 (2018).

[25] Y. Gao, X. Liang, L. A. Dissado, S. J. Dodd, and N. M. Chalashkanov, IEEE Trans. Dielectr. Electr. Insul. **23**, 3683 (2016).

[26] N. G. McCrum, B. E. Read, and G. Williams, *Anelastic and Dielectric Effects in Polymeric Solids* (Wiley, 1967).

[27] F. Kremer and A. Schönhals, *Broadband Dielectric Spectroscopy* (Springer, 2002).

[28] R. M. Hill, L. A. Dissado, and K. Pathmanathan, J. Biol. Phys. **15**, 2 (1987).

[29] R. M. Hill and L. A. Dissado, Solid State Ionics **26**, 295 (1988).

[30] L. A. Dissado and R. M. Hill, Phys. Rev. B **37**, 3434 (1988).